

Rafael E. Carrasquilla⁽¹⁾ and Norman Fitz-Coy⁽¹⁾

(1) University of Florida, PO Box 116250, Gainesville FL 32611-6250

DebriSat: Generating a dataset to improve space debris models from a laboratory hypervelocity experiment

ABSTRACT

Our global dependency on geospatial technologies, communication, and entertainment rely heavily upon spacecraft that are affordable, easily deployable, and increasingly expendable. As of Q4 2019, there are upwards of 5,000 intact spacecraft and 14,000 man-made 10-cm and bigger debris fragments actively tracked as they orbit the Earth. The use of existing spacecraft breakup models to predict the debris fields generated by the Iridium-Cosmos collision in 2009 demonstrated that the models worked well in predicting the debris from the older Cosmos spacecraft but not as well for the more “modern” Iridium spacecraft.

DebriSat is a project conceived to improve orbital environment prediction accuracies by providing data to assist in updating the standard break-up models. The project characterizes fragments resulting from a lab-controlled, hypervelocity collision, involving a 56 kg class spacecraft representative of modern LEO satellites. Fragments with a minimum dimension no less than 2 mm are collected, recorded, analyzed, and archived. Existing breakup models predicted 85,000 fragments to be generated and to date, the DebriSat project has collected approximately 203,000 debris fragments and partially characterized over 70,000 fragments. A significant portion of fragments collected have negligible height in comparison to their other two dimensions, therefore, two fragment size categories were defined: 2D fragments and 3D fragments. Of those characterized fragments, 2D fragments constitute over 98% of the total number of fragments. Conversely, while 2D fragments are more populous, 3D fragments comprise more than 97% of the total characterized mass – approximately 40 kg – of which over 94% is attributed to objects of a metal type. Non-metal or mixed material objects only account for around 6% of all recorded mass to date. This paper discusses the status of the DebriSat project, presents preliminary findings, and highlights some of the challenges and lessons learned during the project.

1. BACKGROUND

In order to improve the accuracy of prediction models for space debris generating events, data from radar observations and controlled tests must be collected, studied, and their findings carefully applied [1-4]. In 1992, one such test, the Satellite Orbital Debris Characterization Impact Test (SOCIT) was performed using a defunct U.S. satellite from the 1960s [5-7]. The results from the SOCIT laboratory hypervelocity impact (HVI) experiment served as the basis for the formulation of standard break-up models used by NASA, the U.S. Department of Defense, and many other agencies with interests in orbital debris [1-4]. While these break-up models performed well initially, certain collision events have since confirmed the models’ debris-prediction accuracies to have an affinity for older satellites and rocket bodies with similar material composition to those of the SOCIT test article – the most notable of these events being 2009’s Iridium-33 and Cosmos-2251 in-orbit satellite collision. Analysis of the post-impact-generated debris cloud demonstrated the break-up model’s accuracy in predicting debris counts for the defunct Cosmos-2251 satellite, as well as its inaccuracies in the prediction of debris from the Iridium-33 satellite. The inconsistencies in the break-up model’s estimates were ascribed to the difference in material composition between the two satellites; fragmentation of the newer components present in Iridium-33 had not been previously studied, and thus were not accounted for in the model [1]. To address the concerns raised by the outdated models’ inaccuracies, NASA and the Department of Defense launched an effort to update the standard break-up model in a manner reflective of the newer materials and components found in modern satellites – the result of which is the ongoing DebriSat project.

The purpose of the DebrisSat project (DebrisSat) is to improve orbital environment prediction accuracies by obtaining the necessary data to update the standard break-up models via detailed fragment characteristics. The test article – a 56 kg spacecraft – was created to be representative of modern low Earth orbit (LEO) satellites by including material components and fabrication processes found in many satellites today and was subjected to an HVI test intended to simulate a catastrophic on-orbit collisions. Following the HVI test, the University of Florida team has continued efforts to collect and characterize the resulting debris fragments in terms of their physical size and shape, mass, material type and properties, bulk density, and ballistic coefficients. With regards to the fragments' physical size, the parameters of interest are their characteristic length (L_c), average cross-sectional area (ACSA), volume, and area-to-mass ratio (AMR).

2. PROJECT OVERVIEW

Whereby previous efforts have focused on the recording of fragment sizes 10 cm and above, the efforts of DebrisSat are focused on the collection, recording, analysis, and archiving of all fragments with a minimum dimension no less than 2 mm. To date there have been in excess of 23,000 in-orbit objects detected by the USAF Space Surveillance Network, from which approximately 20,000 objects are currently tracked and recorded via the U.S. Strategic Command spacecraft catalog, SATCAT [8-10]. The contents of the data catalog as of October 27th, 2019 have been summarized in Table 1. The Payloads category is comprised of all intact on-orbit spacecraft, including those which have a “decommissioned” or “on-standby status” but remain functional. The Debris category consists of non-functional payloads, as well as debris fragments 10 cm or greater in diameter. While the data has been grouped by continent of origin, it is still reflective of the top three sources of space artifacts being the U.S., Russia, and China, respectively. Moreover, when considering the risk potential of untracked debris, along with the untenably disproportionate payloads-to-debris ratios of these top producers, the implications become cause for concern.

As of Q4 2019, the DebrisSat project has characterized over 70,000 debris fragments and collected an excess of 203,000 – approximately a 239% increase from the 85,000-fragment prediction generated by existing breakup models – with active collection efforts remaining ongoing. As seen in Table 2, of these 70,000 characterized debris fragments only around 44,000 have been fully characterized. Given the large volume of remaining fragments expected to be handled, focus is placed on the automation of characterization tasks in order to expedite the process while reducing the risks associated with human error and subjectivity. To that end, the extraction of the parameters associated with size is achieved via automated mass measurement and imaging. Given that a significant portion of the collected fragments have a negligible height when compared to their other dimensions, a threshold was determined, and two size categories were defined: 2D and 3D fragments. In conjunction to the definition of two fragment size categories, two imaging systems – eponymously named the 2D and 3D imaging systems – were created to perform the measurements and calculations associated with the fragments' physical size characterization.

Table 1: Summary of SATCAT On-Orbit Data by Continent of Origin

Source*	Payloads		Debris	All
	On Orbit	Active	On Orbit	On Orbit
Africa	28	17	0	28
North America	1,918	1,081	4,877	6,795
South America	52	34	1	53
Asia	850	623	3,981	4,831
Europe	1,858	361	5,638	7,496
Oceania	20	12	2	22
Other†	595	368	169	764
All	5,321	2,496	14,668	19,989

Note. Data as of Oct. 27th, 2019, *Continental grouping based on countries' self-declared affiliation (e.g. Russia occupies Europe and Asia geographically, but self-recognizes as European), †Includes private organizations, multi-continental partnerships, and artifacts awaiting a source designation

Table 2: Summary of DebrisSat Fragment Counts

Primary Material*	Fragment Counts			Percent Total	
	2D	3D	All	2D	3D
Carbon-Fiber Reinforced Polymer (CFRP)	28,841	68	28,909	99.76%	0.24%
Copper	3,750	25	3,775	99.34%	0.66%
Metal†	3,146	151	3,297	95.42%	4.58%
Epoxy	2,050	107	2,157	95.04%	4.96%
Plastic	1,963	19	1,982	99.04%	0.96%
Aluminum	505	110	615	82.11%	17.89%
Printed Circuit Board (PCB)	555	10	565	98.23%	1.77%
Glass	502	40	542	92.62%	7.38%
Multi-Layered Insulation (MLI)	367	54	421	87.17%	12.83%
Titanium	347	38	385	90.13%	9.87%
Silicon	355	2	357	99.44%	0.56%
Kevlar	300	4	304	98.68%	1.32%
Kapton	237	3	240	98.75%	1.25%
Solar Cell	156	0	156	100.00%	0.00%
Stainless Steel	31	83	114	27.19%	72.81%
Full Characterization	43,105	714	43,819	98.37%	1.63%
Partial Characterization			26,597		
Fragments Characterized			70,416		
Fragments Recorded			178,046		
Fragments Collected			203,000		

Note. *While some fragments include multiple materials, this list only considers the predominant material type for each fragment analyzed, † “Metal” is a placeholder; specific metal types are assigned after verification of density measurements.

3. MEASUREMENT SYSTEMS AND CALCULATIONS

Following the collection and recording of fragments, as well as initial assessment – which includes discernment of material type, shape, and 2D/3D designation – the next phase in the characterization process is the extraction of parameters related to the fragment’s physical size and associated properties (e.g., size dimensions, bulk density, L_c , ACSA, volume, etc.). The first step of this process is to obtain each fragments’ mass measurement, which is done using various calibrated mass balances. As each balance covers different capacity and precision ranges, in order to minimize human error and ensure data integrity, a computer interface was developed to obtain the mass measurements and record them directly to DebrisSat’s database. The interface is set to obtain the measurement data automatically from the balances and record only those which fall under 10% variance of the balance’s re-tare values. If the re-tare value’s variance is greater than 10%, the fragment must be measured again after calibration of the balance before it can proceed to imaging for further size calculations.

The two 2D imaging systems present at DebrisSat (2D imagers 1 and 2) are both comprised of a singular point-and-shoot camera fixed above a staging area with front and back-lit lighting, a glass imaging plate with a metal calibration ring, a 45° angle mirrored prism, a white backdrop, and a computer station (see Figure 1). The metal calibration rings have a 3 mm height-measurement that is commensurate with the experimentally determined threshold used to define 2D and 3D fragments. When placed with a debris fragment on the imaging plate, the calibration ring provides a pixel-to-mm conversion which facilitates the physical size measurement calculations of the three longest orthogonal dimensions denoted as X_{DIM} , Y_{DIM} , and Z_{DIM} . The X-dimension (X_{DIM}) and Y-dimension (Y_{DIM}) of the fragment are extracted from a back-lit image of the fragment and ring, while the Z-dimension (Z_{DIM}) is extracted from the side-view provided by the prism in a front-lit image – the fragment’s L_c is calculated as the algebraic average of these three dimensions. Additionally, the ACSA is calculated as the sum of one-half of the

projected area and one-fourth the surface area of the fragment's perimeter, while the volume is calculated as the projected area multiplied by the fragment's Z_{DIM} .

The 3D imaging system is composed of six point-and-shoot cameras distributed along a vertical arc, a green screen platform and backdrop, three soft-box diffused studio lights, a turntable, and a computer station (see Figure 2). The system uses a space-carving technique to generate a 3D representation of the object to be measured. The vertical arc provides the camera with various vantage points to view the object and assist in space-carving and the generation of a point-cloud. Once the three largest orthogonal dimensions are calculated from the point cloud using a convex hull algorithm, the L_C is derived just as with the 2D imaging system. The volume is determined via an alpha-shape algorithm applied to the point cloud, while the ACSA is calculated from the projected areas of each image used in the space-carving. Additional details on the imaging systems can be observed in [11].

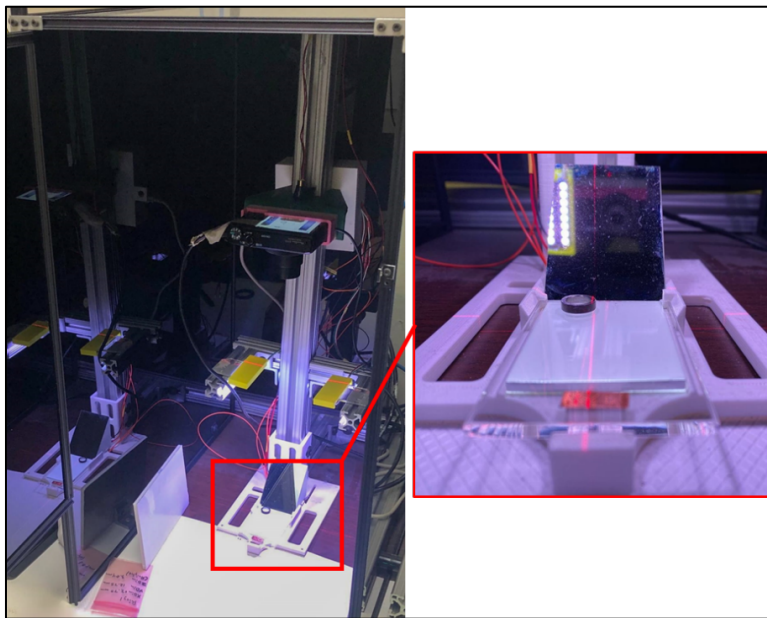


Figure 1: 2D Imaging System Setup



Figure 2: 3D Imaging System Setup

4. PRELIMINARY FINDINGS

Due to the exceptionally high variability of 3D fragments' composition, evaluation of 3D fragment data poses a greater challenge than the analysis of 2D fragment data. While this complexity is partly due the inherent size variability associated with partial restrictions from a defined upper boundary for 2D but not 3D fragments, it is further compounded by a higher rate of multi-material compositions. Currently, the incidence rate of multiple material 3D fragments is 1:3, as opposed to the 1:21 ratio observed in fragments falling under the 2D size category. Furthermore, as the 3D fragment population continues to grow, so too will the magnitude of multi-material fragments and their number of possible permutations. As material properties cannot be isolated from these multi-material fragments, general assumptions about material trends at this time would be tenuous at best, thus fragments must be assessed as a whole unit; pursuant to this, only the predominant material type (defined as "primary material") for all fragments has been considered in this paper.

As of Q4 2019, upwards of 43,000 cataloged 2D fragments have been fully characterized, accounting for over 98% of the total number of fully characterized fragments to date (see Table 2). Conversely, while 2D fragments are more populous, 3D fragments comprise more than 97% of the total characterized mass with a collective 40 kg (see Table 3). This inverse correlation between the magnitude of the fragments' size category and their respective mass, with regards to primary material type, become evident in the side-by-side comparison seen in Figure 3. Apart from the stainless-steel material type, all other materials observe a minority 3D fragment count become a majority mass distribution.

Given prior mention of the considerations required for newer material types, another important item of note for Figure 3 is the distribution comparison of CFRP fragments. Even with a 2D to 3D fragment ratio of 424:1, 3D-CFRP fragment mass accounts for nearly 80% all measured carbon-fiber mass. Nevertheless, CFRP only comprises around 2% of the total 41 kg of characterized mass (see Table 3). Furthermore, of this total characterized mass, over 94% is attributed to objects of a metal type. Non-metal or composite objects - including CFRP - only account for around 6% of all recorded mass to date, despite making up 81% of all characterized fragments (see Table 4).

Table 3: Summary of Recorded DebrisSat Fragment Mass

Primary Material*	Mass (kg)			Percent Total		
	2D	3D	All	2D	3D	All
Metal†	0.6356	35.2608	35.8964	1.77%	98.23%	87.55%
Aluminum	0.0255	1.6862	1.7117	1.49%	98.51%	4.17%
CFRP	0.2061	0.7352	0.9413	21.89%	78.11%	2.30%
Titanium	0.0280	0.4307	0.4587	6.10%	93.90%	1.12%
Stainless Steel	0.0009	0.3804	0.3813	0.24%	99.76%	0.93%
Glass	0.0783	0.2677	0.3460	22.62%	77.38%	0.84%
PCB	0.0270	0.2947	0.3217	8.38%	91.62%	0.78%
MLI	0.0254	0.2043	0.2297	11.06%	88.94%	0.56%
Plastic	0.0680	0.1438	0.2118	32.11%	67.89%	0.52%
Kevlar	0.0004	0.1724	0.1728	0.23%	99.77%	0.42%
Epoxy	0.0168	0.1415	0.1583	10.60%	89.40%	0.39%
Copper	0.0326	0.1071	0.1397	23.34%	76.66%	0.34%
Silicon	0.0027	0.0121	0.0148	18.28%	81.72%	0.04%
Kapton	0.0025	0.0068	0.0093	27.10%	72.90%	0.02%
Solar Cell	0.0018	0.0056	0.0074	24.44%	75.56%	0.02%
Measured Mass	1.1516	39.8494	41.0010	2.81%	97.19%	100.00%

Note. *While some fragments include multiple materials, this list only considers the predominant material type for each fragment analyzed, † "Metal" is a placeholder; specific metal types are assigned after verification of density measurements.

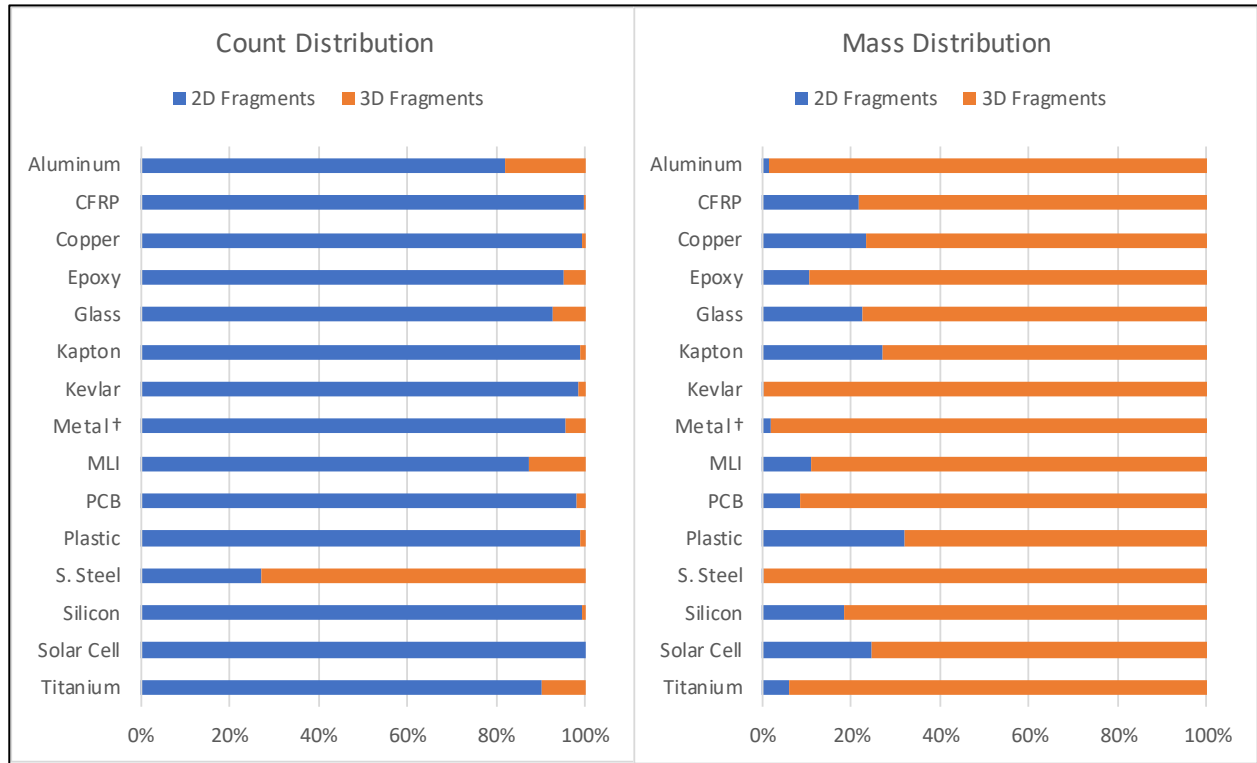


Figure 3: Fragment Distributions per Primary Material Type

Table 4: Summary of Metal v.s. Non-Metal Fragments

Category	Mass in kg (Percent Total)				Total	
	2D		3D			
Metal	0.72	(1.76%)	37.87	(92.35%)	38.59	(94.11%)
Non-Metal	0.43	(1.05%)	1.98	(4.84%)	2.41	(5.89%)
All	1.15	(2.81%)	39.85	(97.19%)	41.00	(100.00%)

Category	Fragment Count (Percent Total)				Total	
	2D		3D			
Metal	7,779	(95.03%)	407	(4.97%)	8,186	(18.68%)
Non-Metal	35,326	(99.14%)	307	(0.86%)	35,633	(81.32%)
All	43,105	(98.37%)	714	(1.63%)	43,819	(100.00%)

5. LESSONS LEARNED

Although the findings discussed in this paper have been discretized to the fragments' primary material types, it is worth noting that certain cases require special considerations in the analysis of data with regards to material types, size, and expected associated characteristics. While further study of the data in Table 3 yields confirmation that metal and 3D-type fragments represent the largest portion of all recorded mass, it also reveals said need for further investigation of special cases. When looking at the percent total values above 90% for the 3D fragment category, all the material-types fall under a metal variety except for PCB and Kevlar. While PCB and Kevlar have the 5th and 6th lowest 3D fragment counts respectively as seen on Table 2, their mass makes up most of each type's total recorded mass.

Being a “soft” type of material primarily used as cable sheathing in DebrisSat, one may not initially expect that Kevlar fragments surviving the HVI test would account for such a relatively high mass percentage when compared to debris fragments of a higher density. However, further investigations reveal how such cases come to pass, as well as the complexities involved with the data analysis of multi-material fragments. Figure 4 shows an example of a characterized 3D-fragment which has been discretized to its primary material type, Kevlar. Although the debris fragment is composed primarily of Kevlar, other material types – including copper, plastic, and CFRP – are clearly visible. Similarly, Figure 5 shows a 3D-fragment which has been discretized to PCB despite the prominent presence of metal standoffs, as well as CFRP.



Figure 4: Side and Top View of a Kevlar 3D-Fragment

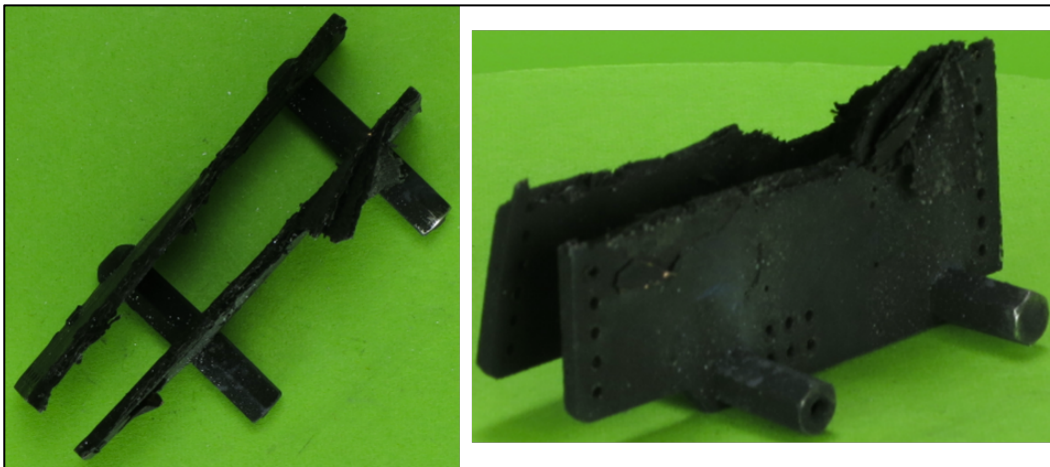


Figure 5: Top and Side View of a PCB 3D-Fragment

At the time of this writing, multi-material fragments make up 46% of all recorded mass (see Table 5). This means that nearly half of the characterization data acquired thus far is comprised of complex geometries and material compositions. While fragments of material types such as epoxy – which was used as an adhesive to bind different material components – are expected to have a higher probability of containing multiple materials, other material types are not as intuitive. Table 5 shows a summary of the distribution of characterized 2D and 3D fragments containing at least two material types. It is further sorted by the percent total of the multi-material fragments’ primary material with respect to all characterized fragments of that same material type.

Following Kevlar, copper and plastic have the 2nd and 3rd highest percent total of multi-material fragments (see Table 5); this means that more often than not, the material types are observed in the presence of other materials. While this is technically true, when observed in multi-material fragments, copper and plastic are almost exclusively found together in the form of wires. When assessing a fragment's material composition, the operator determines the primary material type based on its prevalence. Figure 6 shows a multi-material fragment that has been deemed to be predominantly plastic due to the absence of copper wiring from its plastic sheathing. Conversely, Figure 7 shows a similar fragment for which its primary material has been determined to be copper as a result of the wiring visibly traversing the entirety of the plastic sheathing. Attempts to physically separate the materials in any multi-material fragments would destroy the value of their post-HVI state, while attempts to isolate the individual material properties would prove high impossible – both instances fall outside of the scope of the DebrisSat project.

Table 5: Summary of Characterized Fragments Containing Multiple Materials

Primary Material	2D Multi-Material		3D Multi-Material		All Multi-Material		Percent Total
	Count	Mass (kg)	Count	Mass (kg)	Count	Mass (kg)	
Kevlar	9	0.00003	3	0.17176	12	0.17179	99.42%
Copper	196	0.02090	17	0.09072	213	0.11162	79.88%
Plastic	183	0.06082	4	0.09759	187	0.15841	74.78%
CFRP	1,046	0.06885	42	0.59388	1,088	0.66273	70.41%
Epoxy	213	0.00370	39	0.10766	252	0.11136	70.36%
MLI	14	0.01418	9	0.10723	23	0.12141	52.85%
Metal*	149	0.03058	26	17.00655	175	17.03713	47.46%
Kapton	8	0.00020	0	0.00415	8	0.00435	46.69%
PCB	50	0.00168	5	0.11348	55	0.11516	35.80%
Aluminum	8	0.00038	12	0.46672	20	0.46710	27.29%
Stainless Steel	0	0.00000	12	0.04007	12	0.04007	10.51%
Solar Cell	12	0.00021	0	0.00052	12	0.00073	9.82%
Silicon	18	0.00097	0	0.00035	18	0.00132	8.97%
Titanium	2	0.00003	6	0.02889	8	0.02892	6.30%
Glass	10	0.00011	1	0.01019	11	0.01030	2.98%
All	1,918	0.20264	176	18.83974	2,094	19.04239	46.44%
All Characterized	43,105	1.15158	714	39.84938	43,819	41.00096	100.00%

Note. *Placeholder; Specific metal types are assigned after verification of density measurements.



Figure 6: Top and Side View of Wire Fragment (Plastic)



Figure 7: Top and Side View of Wire Fragment (Copper)

6. CONCLUSION

DebrisSat is a project conceived and operated at an unprecedented scale and scope within the space and orbital debris communities [1, 4-6]. As of Q4 2019, an excess of 203,000 debris fragments have been collected representing a 239% increase from the originally predicted total, with collection efforts remaining ongoing. Of the 203,000 collected fragments, 178,046 have been recorded in DebrisSat's database, and 43,819 have completed characterization. While significant efforts are still required to characterize all collected fragments, the project's primary post-HVI test objective is to recover and characterize 90% of DebrisSat's 56 kg payload mass. To that end, characterization efforts have achieved 82% of the goal, owing to a shift in focus towards the characterization of larger sized fragments.

Lessons learned – past and new – always serve as a guide towards the continuous improvement of existing systems and procedures, as well as perspectives during data analysis. To facilitate expediency and improve calculations while reducing the risks associated with human error and subjectivity, emphasis remains on the automation and further improvements of DebrisSat's measurement systems and procedures. In addition, great time and care must be taken when analyzing the preliminary data obtained to ensure its value for future space missions, policy, and regulations.

7. ACKNOWLEDGEMENTS

The DebrisSat project is funded by the National Aeronautics and Space Administration (NASA) and the United States Air Force/Space and Missile Systems Center (USAF/SMC). The DebrisSat team would like to express their sincere gratitude to NASA and USAF/SMC for their contributions.

8. REFERENCES

- [1] Liou, J.-C., Clark, S., Fitz-Coy, N., Huynh, T., Opiela, J., Polk, M., Roebuck, B., Rushing, R., Sorge, M. and Werremeyer, M., "DebrisSat - A planned laboratory-based satellite impact experiment for breakup fragment characterization," Proceedings of the 6th European Conference on Space Debris, Darmstadt, Germany, 2013.
- [2] Krisko, P. H., Flegel, S., Matney, M. J., Jarkey, D. R., & Braun, V., "ORDEM 3.0 and MASTER-2009 modeled debris population comparison," *Acta Astronautica*, 113, 204-211, 2015.

- [3] Johnson, N. L., Krisko, P., Liou, J.-C. and Anz-Meador, P. D., "NASA's new breakup model of EVOLVE 4.0", *Advances in Space Research*, 28, 1377-1385, 2001
- [4] Watson, E., Maas, H. G., Schäfer, F., & Hiermaier, S., "Trajectory Based 3d Fragment Tracking in Hypervelocity Impact Experiments," *ISPRS-International Archives of the Photogrammetry, Remote Sensing and Spatial Information Sciences*, 422, 1175-1181, 2018
- [5] McKnight, D. S., Johnson, N. L., Fudge, M. L. and Maclay, T. D., "Satellite orbital debris characterization impact test (SOCIT) series data collection report," Kaman Sciences Corporation, Contract No. NA 9-19215, 1995.
- [6] Krisko, P. H., Horstman, M. and Fudge, M. L., "SOCIT4 collisional-breakup test data analysis: With shape and materials characterization," *Advances in Space Research*, 41, 1138 - 1146, 2008.
- [7] Ausay, E., Cornejo, A., Horn, A., Palma, K., Sato, T., Blake, B., Pistella, F., Boyle, C., Todd, N., Zimmerman, J., Fitz-Coy, N., Liou, J.-C., Sorge, M., Huynh, T., Opiela, J., Krisko, P. and Cowardin, H., "A comparison of the SOCIT and DebrisSat experiments," Proceedings of the 7th European Conference on Space Debris, Darmstadt, Germany, 2017.
- [8] Jackson, P. A., "Small satellite debris catalog maintenance issues," Proceedings of the NASA, Lyndon B. Johnson Space Center, 4th Annual Workshop on Space Operations Applications and Research (SOAR 90), 696-704, 1991.
- [9] United States Strategic Command Public Affairs, United States Strategic Command, "USSTRATCOM expands SSA data on Space-Track.org," Available at <https://www.afspc.af.mil/News/Article-Display/Article/1658619/usstratcom-expands-ssa-data-on-space-trackorg/>
- [10] "SATELLITE CATALOG," Available at <https://www.space-track.org/#catalog>, accessed 27 October 2019.
- [11] Shiotani, B., and Fitz-Coy, N., "Imaging Systems for Size Measurements of DebrisSat Fragments," Paper IAC-17.A6.3.6x41656, Proceedings of the 68th International Astronautical Congress, Adelaide, Australia, September 2017.